Preparation and characterization of polyurethane optical phantoms

Theodore Moffitt Yin-Chu Chen Scott A. Prahl

November 9, 2005

Abstract

We describe a method for the preparation of a polyurethane phantom to simulate the optical properties of biologic tissues at two wavelengths in the visible and near infrared spectral range. We characterize the addition of added molecular absorbers with relatively narrow absorption bands (FWHM 32 and 76 nm for Epolight 6084 and 4148 respectively) for independent absorption at 690 nm for absorption up to $5\,\mathrm{cm}^{-1}$ and 830 nm for absorptions up to $3\,\mathrm{cm}^{-1}$. Absorption by both dyes is linear with concentration in these respective regions and is consistent in polyurethane both before and after curing. The dyes are stable over long durations with no more than 4% change. The absorption of visible light by polyurethane decreases with time and is stable by one year with a drop of $0.03 \pm 0.003\,\mathrm{cm}^{-1}$ from 500–830 nm. The scattering properties are selected by the addition of TiO_2 particles to the polyurethane which we functionally describe for the 690 and 830 nm wavelengths as related to the weight per

volume. We demonstrate that the variation in absorption and scattering properties for large batch fabrication (12 samples) is ±3%. The optical properties of the phantoms has not significantly changed in a period of exceeding one year which makes them suitable for use as a reference standard.

keywords: tissue, reflectance, transmission, photostable.

1 Introduction

Phantoms that simulate the optical characteristics of tissues are commonly used to mimic light distributions in living tissue. Tissue phantoms are often designed and utilized for three purposes: to simulate light distributions with a geometry of physical tissue [1], for the calibration of optical devices[2, 3], and for recording a reference measurement with an optical measurement device[4]. For all three uses, the absorption and scattering properties of the created tissue phantom is the primary design factor. Optical tissue phantoms are necessary to calibrate steady-state optical measurements on real tissues to establish quantitative information[3]. Optical device calibration requires using several phantoms with the optical properties that span the typical range of the tissue to be simulated. Furthermore, phantoms that are optically stable are also suitable for use as a reference measurement taken in conjunction with measurements on living tissues.

Several types of phantoms to mimic the optics of human tissue have been described in the literature including homogenized milk [5], non-dairy creamer [6], wax [7], and a blood and yeast suspension [8]. Suspensions of oils/fats in an aqueous solution such as Intralipid

[9] and a water soluble dye (India ink [10]) appear to be the most commonly used phantom materials. Difficulties arise in creating inhomogeneities using liquid phantoms such as layered structure. A desire for solid phantoms led to the development of suspensions of Intralipid and India ink in agar [11], agarose [12] and polyacrylamide [13] that could be cut and shaped to provide inhomogeneities in the phantoms. The inclusion of inhomogeneities limited the selection of dyes used to waterproof inks to prevent diffusion of dyes between regions [11]. However, these phantoms mostly suffer from relatively short useable lifetimes which are usually limited to no more than two months.

More robust phantoms made of rubbers or plastics have been described that give long-term optical stability and greater shaping flexibility. Phantoms compositions of silicone [1, 14], polyester [15, 16], polyurethane [17], and epoxy resin [18] have been described. There may be no great advantage of one material over another. For example, silicone more closely matches the mechanical properties of tissue and may be cast into arbitrary shapes, whereas epoxy, polyurethane, and polyesters are easier to machine after casting. Typically, the selection of a material is determined by the choice of absorbers and their stability in that medium.

The choice of scattering agents in solids is usually limited to aluminum oxide (Al_2O_3) [1, 14], titanium dioxide [15], and silicon dioxide [18, 16], polyester [1], polystyrene, or latex microspheres. Mie theory can be used to predict the scattering properties of microspheres with knowledge of the relative refractive index, size distribution and number density. Unfortunately, microspheres tend to be much more expensive than aluminum oxide or titanium

dioxide particles. One primary difference between aluminum oxide and titanium dioxide particles may be the maximum attainable value for g (the cosine for the mean angle of scattering) which describes the scattering anisotropy; Firbank and Deply found that TiO_2 is limited to $g = 0.7$ whereas Al_2O_3 can reach $g = 0.97$ in polyester resin [15]. Arridge et al. [19] has shown that any arbitrary scattering angle distribution can be theoretically matched using an appropriate distribution of particle sizes.

Our goal was to make durable stable optical phantoms with predefined optical properties at two wavelengths, 690 and 830 nm. To our knowledge, previous phantom designs have been developed for a single wavelength or for use with a single broadband absorbing dye that determines the absorption spectrum. We wanted to use component materials that would be photostable. Moreover, the dyes needed to have absorption spectra with minimal overlap. We encountered two problems during initial material selection experiments. First, dyes that absorb strongly at 830 nm also exhibited comparable absorption at 690 nm and second, dyes that bleached during the curing process of the binding medium. The dyes we selected for our phantoms determined the bulk material used to suspend the dyes and scatterers.

A method is needed to determine the scattering characteristics of the phantoms. Inverse Adding-Doubling (IAD) was used to find the scattering and absorption of a slab of turbid material using total reflection and total transmission measurements. This method is applicable to homogeneous turbid slabs with any optical thickness, albedo, or phase function. The slab may have a different index of refraction from its surroundings and may or

may not be bounded by glass. The optical properties are obtained by iterating an adding-doubling solution of the radiative transport equation until the calculated values of the reflection and transmission match the measured ones. Alternatively, spatially [20, 21, 22] and/or temporally[23, 24, 25] resolved measurements of diffuse light distributions can also be used to quantitatively determine absorption and reduced scattering coefficients.

We present a method for fabricating solid optical tissue phantoms that are castable and photostable. These optical phantoms are designed to be suitable reference standards at two distinct wavelengths and whose optical properties have been carefully measured. The final materials were verified by making several optical phantoms with differing quantities of dye and scattering particles. Phantoms made without added scatterers were made to verify the stability of the dyes' absorption properties before and after the curing process and over a duration of one year.

2 Materials and Methods

2.1 Component material selection

The optical phantoms consist of three components: the polyurethane, the absorbing chromophores, and the scattering agent. Selection of the three primary components were driven by our choice of absorbing dyes.

We used a phthalocyanine (Epolight 6084, Epolin Inc., Newark, NJ) as the absorber at 690 nm. The absorption at 830 nm was achieved using a palladium dye (Epolight 4148).

The dye manufacturer lists these dyes for use in optical filters and laser goggle applications and suggested polyurethane as a casting material. We verified that both dyes lost their absorption during the curing process in epoxy resin (Marine grade epoxy resin, Side A 314 resin and Side B 109 hardener, Tap Plastics, Inc., Dublin CA). Both dyes exhibit narrow absorption bands (FWHM 32 and 76 nm for Epolight 6084 and 4148 respectively) that allow nearly independent absorption at the wavelengths 690 nm by Epolight 6084 and 830 nm by Epolight 4148 when cured in polyurethane (Figure 1). Titanium dioxide (Ti-Pure R-900, Dupont Chemicals, Wilmington, DE) was assumed to behave as a pure scatterer with negligible absorption between 650 and 850 nm. Finally, we used a two part polyurethane system (WC-781 A/B, BJB Enterprises Inc., Tustin, CA) that had a 30 minute pot life to suspend the titanium dioxide and absorbing dyes. This polyurethane is a clear rigid casting resin that is designed to be tintable and pigmentable. This polyurethane is formed by mixing part "A" with part "B" in a ratio of 100/85 by weight (100/88 by volume). The pot life for the polyurethane was a convenient duration because it allowed sufficient time to mix and de-gas but still cured quickly enough that no apparent settling of the scatterers took place. The viscosity of the mixed polyurethane is 650 cps. The demolding time is 24 hours. Optical measurements could be made at 24 hours. However, complete curing of the polyurethane requires 5-7 days at room temperature or 16 hours at 71–82 degrees C.

2.2 Initial studies

2.2.1 Absorber characterization

The absorption coefficients as a function of dye concentration were measured in cured polyurethane (WC-781 A/B, BJB Enterprises Inc., Tustin, CA). Stock solutions of the two powdered dyes were prepared in xylene with concentrations of 6.64 mg/mL of Epolight 6084 and 1.56 mg/mL of Epolight 4148. Stock solutions of the dyes were pipetted and mixed in 5 quantities of 15, 25, 35, 40, and 45 μl of Epolight 6084 stock into 10 ml of polyurethane part A and 5 quantities ranging 50 to 250 μl in 50 μl increments of Epolight 4148 stock into 8.8 ml of polyurethane part B. The absorbance of each concentration of Epolight 6084 in part A was measured using a dual beam Cary 100 Bio Spectrophotometer (Varian Scientific Instruments Inc., Walnut Creek, CA) with a cuvette of polyurethane part A in the path of the reference beam. Likewise, the absorbance of Epolight 4148 for each concentration was measured with a cuvette of polyurethane part B in the reference beam path. Then the two parts of the polyurethane were randomly combined with the concentration of dye in part A randomly assigned to each concentration of dye in part B. The samples are thoroughly mixed together and poured into 1 cm cuvettes. Degassing of the mixtures was performed by placing the samples into a desiccator/vacuum chamber (Nalgene 5311 desiccator, Nalge Nunc International, Rochester, NY) that was connected to a vacuum pump (Speedivac 2, Edwards High Vacuum Int., England) capable of reducing the pressure to less than 1 mbar. After full curing, the absorbance of the cuvettes was measured on the Cary spectrometer. These measurements used polyurethane without added absorbers cured in an identical cuvette in

the reference beam path.

A difference of absorbance measurements with the Cary spectrophotometer were used to determine the absorption coefficient of polyurethane. Two samples of polyurethane were cast without any added absorbers, one as a thin slab and another as a tall cylinder. After 48 hours of curing, the samples were removed from their respective molds. The surfaces of each sample was hand polished starting with 9 micron grit aluminum oxide sandpaper (AngstromLap, Fiberoptic Center, Inc., New Bedford, MA) and finishing with 0.3 micron grit paper to create an optically smooth surface. The final thickness of the slab and cylinder of polyurethane were respectively 0.41 and 3.44 cm. The difference between the two samples relative to air (i.e. nothing in the reference beam path) produced a lower noise signal than when the thin slab was placed in the reference arm of the spectrometer and the cylinder in the sample arm.

2.2.2 Titanium dioxide scattering

A stock solution of titanium dioxide consisted of 20.0 grams of titanium dioxide suspended in 60 mL ethanol. Before dilution into the polyurethane, the titanium dioxide stock solution was shaken by hand then sonicated for at least five minutes to ensure complete suspension of TiO_2 particles. To test the scattering coefficients of different concentrations of titanium dioxide in polyurethane, we added different amounts of TiO_2 stock solution into polyurethane in two separate batches. The first batch had two samples with a TiO_2 concentrations of 2.5 and 5 mg/ml; we added 3.84 μg/ml of Epolight 6084 dye and 3.11 μg/ml of Epolight 4148 dye for final absorption coefficients, $\mu_a^{690} = 0.74\,\mathrm{cm}^{-1}$ and $\mu_a^{830} = 0.19\,\mathrm{cm}^{-1}$ to both samples. For

the second batch consisting of two samples with TiO_2 concentrations of 0.5 and 1 mg/ml, we added 7.69 μg/ml of Epolight 6084 dye and 1.56 μg/ml of Epolight 4148 dye for final absorption coefficients, $\mu_a^{690} = 1.17\,\mathrm{cm}^{-1}$ and $\mu_a^{830} = 0.11\,\mathrm{cm}^{-1}$ to each sample. From each sample in both batches, a small portion of the final mixture was poured into a weighing boat, degassed for about 8 minutes. This provided a thin disk used for the inverse Adding-Doubling method. The Inverse Adding-Doubling (IAD) method (described in a later section) was used to characterize the scattering coefficient for each of the above samples.

Scanning electron microscopy was used to evaluate the size distribution of the TiO_2 particles. Three samples were prepared by diluting the stock solution of TiO_2 with additional ethanol. A 5 μl drop of the diluted stock was pipetted onto a clean microscope cover slip and allowed to evaporate leaving a film of TiO_2 particles. The horizontal width of 112 randomly selected particles was measured from 5 separate SEM images using ImageJ software. The scale bar was used to establish the width of a pixel within each image.

2.3 Phantom design

Our two wavelength phantoms had four variables to specify (μ_{a,λ_1}, μ_{a,λ_2}, μ'_{s,λ_1}, and μ'_{s,λ_2}) but only three free parameters since the reduced scattering coefficients at the two wavelengths are related by the use of a single scattering agent. In other words, we could select the optical properties at the first wavelength but the reduced scattering at the second wavelength has a constant proportional relationship to the reduced scattering at first wavelength with respect to scatterer concentration. To compensate, we condensed the desired optical properties into

three parameters μ_{a,λ_1}, μ_{a,λ_2}, and the reduced albedo at the second wavelength (a'_{λ_2}). The reduced albedo was defined by

$$a'_{\lambda_2} = \frac{\mu'_{s,\lambda_2}}{\mu_{a,\lambda_2} + \mu'_{s,\lambda_2}}$$

The desired absorption and reduced scattering properties at the second wavelength (830 nm) would be modified by the following method which kept the reduced albedo constant for $\lambda 2$. A flow chart of this process was diagrammed in figure 2. The wavelength dependence of the reduced scattering coefficient for our TiO_2 particles was determined using IAD and fit by the equation $\mu'_s = (7.0\,\mathrm{cm}^{-1})(\frac{\lambda}{690\,\mathrm{nm}})^{-0.8}$. The effective reduced scattering coefficient at 830 nm was calculated given the desired reduced scattering coefficient at 690 nm. The modified absorption coefficient was calculated using the desired reduced albedo and the dependent reduced scattering coefficient at 830 nm.

2.4 Fabrication method of tissue phantoms

The optical properties of the tissue phantoms were chosen to represent a range of different optical properties at the 690 and 830 nm wavelengths. The absorption coefficient at these two wavelengths would be varied to correspond to physiologic relevant values for the sum total of contributions by a fractions of water, oxygenated and deoxyhemoglobin and a wavelength constant background absorption. For all the phantoms, the scattering coefficient would be held constant. However, the wavelength dependence of the scattering from TiO_2 differs from tissue in that the ratio of scattering coefficients at 690 nm to 830 nm for TiO_2 does not equal the target ratio for tissue. To account for this effect, the target absorption coefficients at

830 nm were adjusted as described in the previous section. Finally, a single set of optical properties was used to make twenty identical phantoms.

The sequence for phantoms preparation was as follows using the stock solutions of dye and TiO_2 described above. We made cylindrically-shaped phantoms 7 cm in diameter and about 5 cm in height. This corresponded to ∼200 mL polyurethane by mixing 113.4 g of part A and 97 g of part B. In addition, an extra 5.3 g of part A and 4.5 g of part B was prepared for making thin slab for optical property characterization. The proportions of each part of polyurethane was determined by weight and the addition of either dye or TiO_2 were neglected since their contribution was less than 1 part in 200 for all phantoms. Absorbers were added to the polyurethane in part A while the scatterers were mixed to part B. Since the scattering of all phantoms were to be identical, 11 ml of TiO_2 stock was mixed into 2628 g of part B polyurethane which was sufficient quantity for all phantoms.

Part A of the polyurethane (118.8 g) was weighed out for a single phantom into a polyethylene container. Stock of Epolight 4148, the near-infrared dye was first pipetted into part A and stirred in with a glass rod until visibly homogenous. This dye had a pale violet tint when mixed into the polyurethane but was not noticeable after the addition of the Epolight 6084 stock which produces a strong turquoise blue tint. When both dyes are homogeneously stirred into part A, about 2 ml was placed in a cuvette for an absorbance measurement on the Cary Spectrometer using a cuvette of part A polyurethane without dye in the reference arm to verify proper absorption attenuation.

At this point, 5.3 g of the part A with dye was set aside in a plastic weigh boat dish.

The remaining portion of polyurethane part A with dye was weighed again to calculate the appropriate quantity of the part B with TiO_2 to be added by weight. While on the scale, part B was poured into part A. The final amount of Part B was added drop by drop using a wooden tongue depressor. The large flat area of the tongue depressor allowed drops to be controlled so that weight of any drops could be controlled with precision of about 0.03 g. The polyurethane is thoroughly mixed using a tongue depressor to scrape the container sides/bottom and stir for about 2 minutes. Most of the mixture was then poured into 16 oz. HDPE molds (16 oz specimen containers, Fisher Scientific International, Inc., Fair Lawn, NJ). The remaining material was poured into two plastic weighing-boats to cast thin disks of differing thickness and about 6 cm in diameter. The set aside 5.3 g of polyurethane part A and dye was treated identical as above, except it had 4.5 g of transparent part B added to it. Also these samples were mixed then poured into 1 cm pathlength cuvettes for casting.

It was necessary to remove entrapped bubbles in the polyurethane introduced by the mixing of components together. Up to five phantoms or weigh boat slabs could be degassed at a time. This restricted us to mixing no more than two sets of optical properties together at a single time since for each set, a phantom and two slabs were made. The second second set was mixed while the first set was degassing. Degassing was done by placing the samples in a desiccator/vacuum chamber (Nalgene 5311 desiccator, Nalge Nunc International, Rochester, NY). The chamber was connected to a vacuum pump (Speedivac 2, Edwards High Vacuum Int., England) capable of reducing the pressure to less than 1 mbar. Samples were degassed for about 8 minutes at which time bubbles stopped forming.

After degassing, the phantoms were set onto a level surface and covered. The phantoms were solid after 24 hours and could be removed from the mold. However at 24 hours, the polyurethane is relatively soft, such that fingerprints can be embedded on the surface with moderate pressure. In general, we waited 48 hours before removing the samples from the casting mold. The phantoms in the specimen container molds were removed by flexing the walls of the container and then pushing on the bottom while holding the phantom upside down. The samples cast in weigh boats were removed by peeling the weigh boat which tore away from the polyurethane.

The phantoms were finished by leveling the top surface of the polyurethane block. A lathe was used to mill the meniscus lip from the top of each phantom until the shiny surface was completely removed. Then each phantom was sanded by hand in two steps: rough finishing with 200 grit wet sandpaper and fine finishing with 600 grit wet sandpaper. In each sanding step, the paper was wet with water and placed on a glass surface while the polyurethane block was sanded in a circular motion. Elimination of visible surface scratches were used as a completion condition.

2.5 Testing of phantom optical properties

Absorption of each phantom was measured using the Cary spectrometer 48 hours after casting. The clear samples cured in cuvettes for each phantom were measured referenced to cured polyurethane without dyes in a cuvette. Four absorbance measurements of each sample were recorded. Additional measurements of the same cuvette samples were recorded

1 year later to establish long term stability.

Inverse Adding-Doubling (IAD) was used to find the scattering and absorption of a slab of turbid material using total reflection and total transmission measurements. Two measurements on each of the two thin slabs for each phantom were made. Total diffuse reflection measurements were made using an 203.2 mm diameter integrating sphere (IS-080-SF, Labsphere, Inc., North Sutton, NH) with a 12.7 mm diameter detector port and a 31.75 mm diameter sample port with a baffle between ports. Light was guided to the phantom disk through a 400 micron diameter optical fiber (0.22 numerical aperture) placed about 4 mm above the sample centered with the port hole. A 4 mm diameter steel tube coated with multiple coats of flat white paint was used to sleave the fiber through a 6.35 mm top port down to the phantom disk. An Oriel mercury lamp was used for the source and a 600 micron diameter (0.38 numerical aperture) delivered light from the integrating sphere to a scanning grating detector system of a Fluorolog-3 spectrofluorometer (Instruments S.A., Inc., Edison, NJ). The detector fiber was connected to the integrating sphere using an SMA connector surrounded by white shielding in the 12.7 mm port. Measurements were referenced to a 99% Spectralon reflectance standard (Labsphere, Inc., North Sutton, NH) and a dark measurement where the sample port was open and the fiber illuminating black felt on the optical table 254 mm below the port. Four measurements were made on each disk; two measurements on each side. The phantom disks were placed flush with the sample port. Figure 3 shows the sphere measurements for total reflection and figure 4 shows the reference sphere calibration measurements.

Total diffuse transmission measurements were made with another identical integrating sphere. In this set-up only two ports were open, the 25.4 mm diameter sample port and 12.7 mm diameter detector port with a baffle between ports. For this arrangement, the phantom disk was placed on the top port and light was collected with the same detector 600 micron diameter fiber we previously described. Light was delivered to the phantom disk with the 400 micron fiber. The end of the fiber was positioned just above the phantom disk ($<$ 1 mm) centered with the port hole. Again, four measurements were recorded on each disk; two measurements on each side. Measurements were referenced to 100% with the fiber illuminating the open port hole and a dark measurement with an open port but the fiber removed from the sample porthole. Figure 5 shows the sphere arrangement for total diffuse transmission measurements.

Two other values were needed to calculate the scattering properties. The thickness of each phantom disk was measured using a depth gage (ID-C112EB, Mitutoyo Corp. Japan). The refractive index of the cured polyurethane was measured at 670 nm using an Abbé refractometer as 1.468. We assumed negligible change in the refractive index over the spectral range of 500 to 900 nm.

The total diffuse reflectance and transmittance measurements in terms of percentage at all wavelengths were input into the IAD program. The total diffuse reflection was calculated using

$$r_{sample} = \frac{P_{sample} - P_0}{P_{std} - P_0}$$

The total diffuse transmission was calculated using

$$t_{sample} = \frac{P'_{sample} - P'_0}{P'_{std} - P'_0}$$

The batch variability was measured on twelve out of twenty phantoms from a single batch to establish the variability in our fabrication method. A thin slab was cut and sanded flat from twelve of the phantoms. The thickness of each slab was measured with a depth gage. Total diffuse reflection and transmission measurements were recorded for each of the twelve slabs along with reference measurements as previously described. Inverse adding-doubling was used to determine the absorption and reduced scattering coefficient for each slab over the wavelength range of 650–850 nm.

3 Results and Discussion

3.1 Absorption characterization

Both dyes exhibit stable absorption properties in polyurethane after a period of 14 months from casting. The visible/NIR spectra for the absorption coefficient of Epolight 6084 and 4148 is shown in figure 1. Figure 6 shows the absorption coefficient at 690 and 830 nm as related to the concentration of Epolight 6084 and 4148, respectively. The absorption coefficient at 690 nm relates only to the concentration of Epolight 6084 (C_{6084}) by the relation

$$\mu_a^{690} = a_1 C_{6084} + \mu_{a0}^{690} \tag{1}$$

where $a_1 = 0.16\,\mathrm{cm^{-1}mL/\mu g}$ and $\mu_{a0}^{690} = 0.019\,\mathrm{cm^{-1}}$ when the Epolight 4148 is present at a concentration less than $21\,\mu\mathrm{g/mL}$. Likewise when Epolight 6084 is less than $16\,\mu\mathrm{g/mL}$, the absorption coefficient at 830 nm depends solely on the concentration of Epolight 4148 (C_{4148}) by the linear relation

$$\mu_a^{830} = a_2 C_{4148} + \mu_{a0}^{830} \tag{2}$$

where $a_2 = 0.065\,\mathrm{cm^{-1}mL/\mu g}$ and $\mu_{a0}^{830} = 0.013\,\mathrm{cm^{-1}}$. The linear relations for the absorption coefficient are applicable for Epolight 6084 up to a concentration of at least $32\,\mu\mathrm{g/mL}$ and for Epolight 4148 up to $45\,\mu\mathrm{g/mL}$. A comparison of the absorption from each dye in solution in one part of the polyurethane and then after casting is shown in figure 7 for Epolight 6084 and figure 8 for Epolight 4148. The absorption spectra of both dyes was unaffected by curing.

The tissue phantoms are limited by a minimum intrinsic absorption coefficient that is due to the absorption the of the binding medium. The absorption coefficient of polyurethane at a time point one week after casting is greater than after 13 months from casting as shown in figure 9. The change of absorption at these time points is $0.03 \pm 0.003\,\mathrm{cm^{-1}}$ over the wavelength range of 500–835 nm. The polyurethane absorption is stable between 13 and 14 month time points, but it is not known how gradual or when exactly the drop in absorption occurred between the one week and 13 month time points. The polyurethane exhibited less absorption than two other resins (an epoxy resin and a polymer resin) which showed significant absorption occurring below 500 nm thus giving each a yellow tint as shown in figure 10.

3.2 Scatterer characterization

The scattering coefficients were determined from diffuse reflection and transmission measurements. A typical spectra is shown in figure 11. This illustrates the wavelength separation in the absorption of the two dyes in the reflected and transmitted light. The noise above 850 nm is a consequence of lower power from the lamp at longer wavelengths and lesser efficiency of the photomultiplier tube above 800 nm. The reduced scattering coefficient as a function of wavelength (figure 12) was obtained using inverse adding-doubling using the total diffuse reflection and transmission measurements shown in figure 11. For comparison, the absorption coefficient obtained from a spectrometer measurement of a sample without titanium dioxide is also shown. The reduced scattering coefficient, μ_s' relates to the scattering coefficient (μ_s) and the cosine of the mean angle of scattering (g) from the incident direction of light by the equation $\mu_s' = (1 - g)\mu_s$. The reduced scattering coefficient is an equivalent optical parameter that is one over the mean free path between scattering events when the scattering phase function is isotropic. Since, two measurements are recorded, only absorption and the reduced scattering coefficient can be determined. The anisotropy and the scattering coefficient, μ_s were not determinable separately with another measurement of ballistic photons. Our slabs (ranging from 2–7 mm) were sufficiently thick that all transmitted light was completely diffuse.

The derived scattering properties for the titanium dioxide are shown in figure 13. From this plot, one can predict the scattering coefficient for various concentrations of titanium

dioxide which follows the relations

$$\mu'_{s,690} = a_3 C \tag{3}$$

$$\mu'_{s,830} = a_4 C \tag{4}$$

where $a_3 = 8.0\,\mathrm{cm}^{-1}\,\mathrm{mL/mg}$, $a_4 = 6.61\,\mathrm{cm}^{-1}\,\mathrm{mL/mg}$ and C is the concentration of the titanium dioxide. It is seen that the scattering coefficient is linear with concentration. The different slopes correspond to the altered scattering efficiencies of the titanium dioxide particles at 690 and 830 nm. The size distribution of the titanium dioxide particles is shown in figure 14 having a mean of 340± 90 nm. If we approximate the particles as spheres, then Mie theory can be used to predict the scattering anisotropy for the average particle size. Three-fourths of all particles were between 250 and 400 nm in diameter, and so the average value of g in 10 nm increments across this range is $g = 0.51$ at 690 nm and $g = 0.52$ at 830 nm.

3.3 Phantom optical properties

A set of ten optical phantoms were made with differing levels of absorption but with the same scattering properties. The variation among the ten phantoms in the scattering coefficient at 690 and 830 nm is shown in figure 15. Typical absorption spectra for three of the ten differing phantoms are shown in figure 16. The measured absorption coefficients at 690 and 830 nm of the ten samples are shown relative to the predicted absorption from equations 1 and 2 in figure 17. The difference between predicted and the measured absorption coefficients for the ten phantoms was plus or minus 3 percent at 690 nm and 6 percent at 830 nm.

The reproducibility of a phantom with a single set of absorption and scattering properties is shown in figures 18 for twelve phantoms made from a single batch. Both absorption and scattering varied by plus or minus 3% between 600 and 800 nm. Between 500 and 600 nm, the percentage absorption variation increases but the absolute error remains constant. At wavelengths longer than 800 nm, the error increased (as previously stated) due to lamp power and decreased detector efficiency. Since both the Epolight 6084 and 4148 were mixed together in one part of the polyurethane and titanium dioxide to the other part before combining the two parts, the actual percentage variation in absorption at 830 nm should be comparable to that at 690 nm. Since all twenty phantoms come from a single large batch where all the dye was added to Part A of the polyurethane and the TiO_2 was added to part B for all twenty samples, then the variation in the samples can only come from 2 sources: weighing errors for the combination to the two parts of polyurethane or inhomogeneities in our large solutions of components. The largest weighing error was less than 2% for all phantoms including the ten with different absorption properties.

To minimize error due to inhomogeneities, the part of the polyurethane with TiO_2 was regularly stirred to prevent settling of the scatterers before mixing with the part with the added absorbers. However after combining the two parts of the polyurethane together, the phantom cannot be stirred once the degassing step begins. Samples were held under vacuum at a minimum of eight minutes but may be degassed for 10-12 minutes. Though the pot life of the polyurethane was an hour, by 30 to 45 minutes the polyurethane was warm and noticeably beginning to gel. It is doubtful that full degassing of phantoms can be performed

with a pot-life less than half an hour since gelling of the polyurethane will inhibit gas from escaping. It took about 5 hours to make all twenty phantoms with two people working. The timeliest part of the process was degassing because we were limited to only 4 or 5 phantoms in a vacuum chamber due to space constraint.

4 Conclusions

We presented a method to fabricate tissue phantoms that simulate the optical properties of living tissue at the 690 and 830 nm wavelengths. The optical properties of the phantoms has been consistent in a period that of 14 months from the date of casting. The two molecular dyes provided independent absorption between our chosen wavelengths for absorption coefficients up to 5 and 3 cm^{-1} at 690 and 830 nm respectively. These dyes exhibited stable absorption through the curing process of polyurethane. In addition, the high molecular extinction coefficient of each dye allowed us to keep the addition of dye stock to less than 0.1 percent of the volume of the polyurethane. The polyurethane itself was the only component that changed after casting. The absorption due to the polyurethane decreased approximately by a factor of 2 over the visible spectrum. This change is assumed to occur gradually though we don't have evidence to support this belief. Though polyurethane slowly changes absorption properties, the effect is to make the material more colorless which help to make any added dyes the more dominant absorber.

Polyurethane as a phantom material was easy to work with and handle. The material becomes solid by 24 hours after mixing but is not fully cured. We found that the polyurethane

could not be machined for at least 48 hours. Even sanding of the material before 48 hours is futile because ripples would form on the surface. This polyurethane may be cast into any shape but the material of the mold determines how easy it is to extract the polyurethane after curing. Polyethylene containers readily released after curing. Attempts to cast the polyurethane between glass slides proved more problematic. Spray on mold release (Ease Release 400, Mann Formulated products, Easton, PN) allowed the polyurethane to release from glass but the thin film of mold release caused surface roughness to the polyurethane making it like frosted glass. Polycarbonate molds behaved more like glass in terms of demolding. The mold release allowed polyvinylchloride (pvc) pipe to act as a mold too, but only the polyethylene worked well without the mold release.

Degassing of the polyurethane was a necessary though time-consuming step in the phantom preparation. Significant bubble formation occurs during each mixing step. For our phantoms at least three mixing steps occurred for each phantom, since we had two dyes and the two components of polyurethane. Bubbles that are not removed provide many inhomogeneities, and may act as large scatterers. Removal of the bubbles allows for consistency in the finished product that otherwise would not be obtainable.

We determined four linear relationships (eqs. 1–4) that describe the the absorption coefficient as a function of dye concentration and the reduced scattering coefficient as a function to the titanium dioxide concentration. These relationships predicted the measured absorbing and scattering properties with less than 4% error. The optical properties of the phantoms have shown to be stable over a period of 14 months making the phantoms suitable for use

as reference standards.

References

[1] R. Bays, G. Wagnieres, D. Robert, J. Theumann, A. Vitkin, J. Savary, P. Monnier, and H. van den Bergh, "Three-dimensional optical phantom and its application in photodynamic therapy," *Lasers Surg. Med.*, **vol. 21**, pp. 227–234, 1997.

[2] P. R. Bargo, S. A. Prahl, S. L. Jacques, "Optical properties effects upon the collection efficiency of optical fibers in different probe configurations," *IEEE J. S. T. Q. E.*, **vol. 9**, pp. 314–321, 2003.

[3] G. Zonias, L. T. Perelman, V. Backman, R. Manahoranm, M. Fitzmaurice, J. Van Dam, and M. S. Feld, "Diffuse reflectance spectroscopy of human adenomatous colon polyps *in vivo*," *Appl. Opt.*, **vol. 38**, pp. 6628–37, 1999.

[4] P. R. Bargo, S. A. Prahl, S. L. Jacques, "Collection efficiency of a single optical fiber in turbid media," *Appl. Opt.*, **vol. 42**, pp. 3187–97, 2003.

[5] B. Wilson, Y. Park, Y. Hefetz, M. Patterson, S. Madsen, and S. Jacques, "The potential of time-resolved reflectance measurements for the noninvasive determination of tissue optical properties," *Proc. SPIE*, **vol. 1064**, pp. 97–106, 1989.

[6] J. Linford, S. Shalev, and J. Bews, "Development of a tissue equivalent phantom for diaphanography," *Med. Phys.,*, **vol. 13**, pp. 869–875, 1986.

[7] B. C. Wilson, T. J. Farrell, and M. S. Patterson, "An optical fiber based diffuse reflectance spectrometer for noninvasive investigation of photodynamic sensitizers *in vivo*," *Proc. SPIE*, **IS6**, pp. 219–232, 1990.

[8] B. Chance, J. Haselgrove, N-G. Wang,M. Maris, and E. Sevick, "Photon dynamics in tissue imaging," *Proc. SPIE*, **Vol. 1525**, pp. 68–82, 1991.

[9] S. T. Flock, S. L. Jacques, B. C. Wilson, W. M. Star, and M. J. .C. van Gemert, "Optical properties of Intralipid: a phantom medium for light propagation studies," *Lasers Surg. Med.*, **vol. 12**, pp. 510–519, 1992.

[10] S. J. Madesn, M. S. Patterson, and B. C. Wilson, "The use of India ink as an optical absorber in tissue-simulating phantoms," *Phys. Med. Biol.*, **vol. 37**, pp. 985–993, 1992.

[11] R. Cubeddu, A. Pifferi, P. Taroni, A. Torricelli, and G. Valentini, "A solid tissue phantom for photon migration studies," *Phys. Med. Biol.*, **vol. 42**, pp. 1971–1979, 1997.

[12] G. Wagnieres, S. Cheng, M. Zellweger, N. Utke, D. Braichotte, J. Ballinni, and H. van den Bergh, "An optical phantom with tissue-like properties in the visible for use in PDT and fluoescence spectrosopy," *Phys. Med. Biol.*, **vol. 42**, pp. 1415–1426, 1997.

[13] M. N. Lizuka, M. D. Sherar, and I. A. Vitkin, "Optical phantom materials for near infrared laser photocoagulation studies," *Lasers Surg. Med.*, **vol. 28**, pp. 237–243, 2001.

[14] M. Lauldi, A. Colombo, B. Farina, S. Tomatis, and R. Marchesini, "A phantom with tissue-like optical properties in the visible and near-infrared for use in photomedicine." *Lasers Surg. Med.*, **vol. 28**, pp. 237–243, 2001.

[15] M. Firbank and D. T. Delpy, "A design for a stable and reproducible phantom for use in near infra-red imaging and spectroscopy," *Phys. Med. Biol.*, **vol. 38**, pp. 847–853, 1993.

[16] U. Sukowski, F. Shubert, D. Grosenick, and H. Rinneberg, "Preparation of solid tissue phantoms with defined scattering and absorption properties for optical tomography." *Phys. Med. Biol.*, **vol. 41**, pp. 1823–1844, 1996

[17] M. L. Vernon, J. Frechette, Y. Painchaud, S. Caron, and P. Beaudry, "Fabrication and characterization of a solid polyurethane phantom for optical imaging through scattering media," *Appl. Opt.*, **vol. 38**, pp. 4247–4251, 1999.

[18] M. Firbank, O. Motaki, and D. T. Delpy, "An improved design for a stable and reproducible phantom for use in near infra-red spectroscopy and imaging," *Phys. Med. Biol.*, **vol. 40**, pp. 955–961, 1995.

[19] S. R. Arridge, P. van der Zee, D. T. Delpy, and M. Cope, "Particle sizing in the Mie scattering region: singular value analysis," *Inverse Problems*, **vol. 5**, pp. 671–689, 1989.

[20] T. J. Farrell, M. S. Patterson, and B. C. Wilson, "A diffusion theory model of spatially resolved, steady-state diffuse reflectance for the noninvasive determination of tissue optical properties *in vivo*," *Med. Phys.*, **vol. 19**, pp. 879–888, 1992.

[21] R. Bays, G. Wagnieres, D. Robert, D. Braichotte, J. F. Savary, P. Monnier, and H. van den Bergh, "Clinical determination of tissue optical properties by endoscopic spatially resolved reflectometry," *Appl. Opt.*, **vol. 35**, pp. 1756–1766, 1996.

[22] A. Kienle, L. Lilge, M. S. Patterson, R. Hibst, R. Steiner, and B. C. Wilson, "Spatially resolved absolute diffuse reflectance measurements for noninvasive determination of the optical scattering and absorption coefficients of biological tissue," *Appl. Opt.*, **vol. 35**, pp. 2304–2314, 1996.

[23] J. B. Fishkin, O. Coquoz, E. R. Anderson, M. Brenner, and B. J. Tromberg, "Frequency-domain photon migration measurements of normal and malignant tissue optical properties in a human subject," *Appl. Opt.*, **vol. 36**, pp. 10–20, 1997.

[24] B. J. Tromberg, O. Coquoz, J. B. Fishkin, T. Pham E. R. Anderson, J. Butler, M. Cahn, J. D. Gross, V. Venugopalan, and D. Pham, "Noninvasive measurements of breast tissue optical properties using frequency-domain photon migration," *Philos. Trans. R. Soc. London Ser.*, B **352**, pp. 661–668, 1997.

[25] G. Mitic, J. Kölzer, J. Otto,E. Plies,G. Sölkner, and W. Zinth, "Time-gated transillumination of biological tissues and tissue-like phantoms," *Appl. Opt.*, **vol. 33**, pp. 6699–6710, 1994.

[Figure 1 about here.]

[Figure 2 about here.]

[Figure 3 about here.]

[Figure 4 about here.]

[Figure 5 about here.]

[Figure 6 about here.]

[Figure 7 about here.]

[Figure 8 about here.]

[Figure 9 about here.]

[Figure 10 about here.]

[Figure 11 about here.]

[Figure 12 about here.]

[Figure 13 about here.]

[Figure 14 about here.]

[Figure 15 about here.]

[Figure 16 about here.]

[Figure 17 about here.]

[Figure 18 about here.]

List of Figures

List of Figures

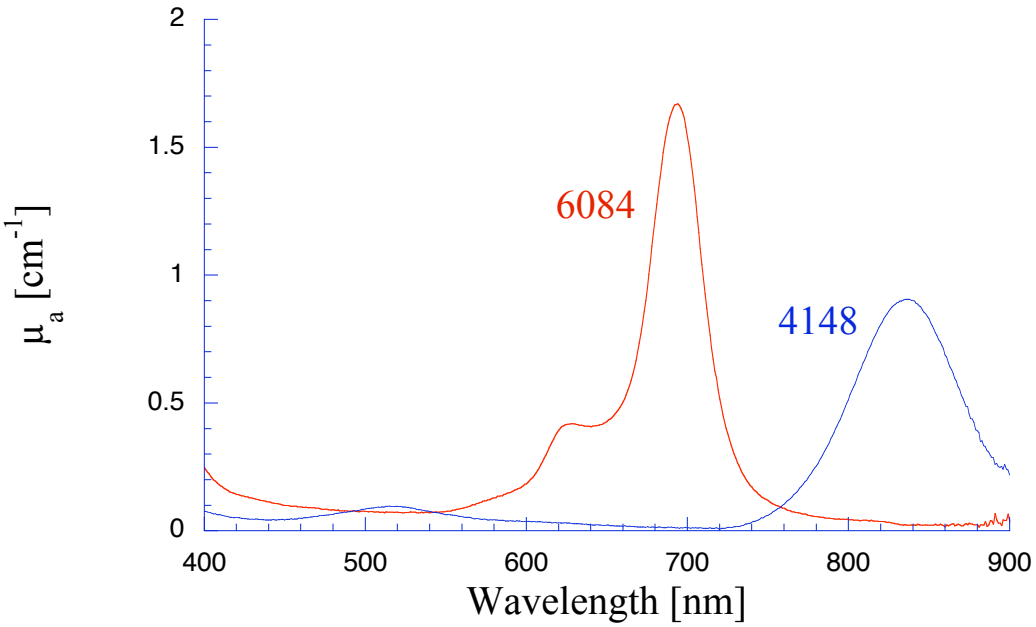

Figure 1: The absorption coefficient spectra of 10 μg/mL Epolight 6084 in polyurethane and 17 μg/mL Epolight 4148 in polyurethane.

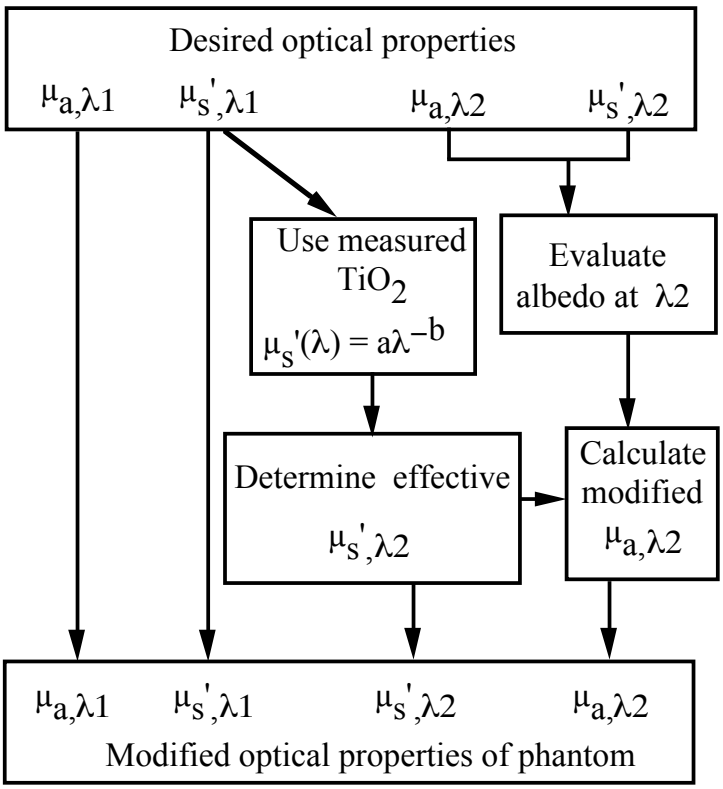

Figure 2: Process for maintaining the four desired optical properties with only three independent variables. The reduced scattering of the first wavelength establishes the reduced scattering at the second wavelength. A new absorption coefficient is calculated at the second wavelength that holds the desired reduced albedo at the second wavelength constant relative to the new optical properties.

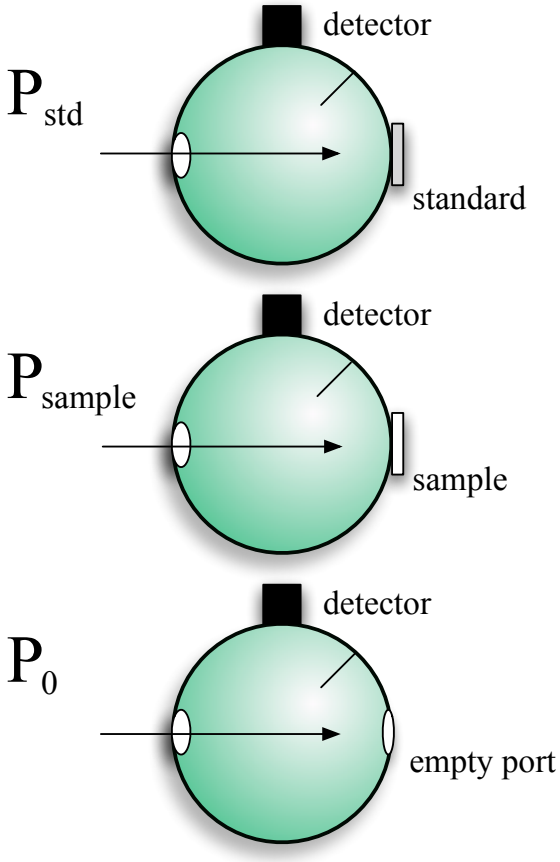

Figure 3: Diagrams of various integrating sphere reflectance measurements that are needed.

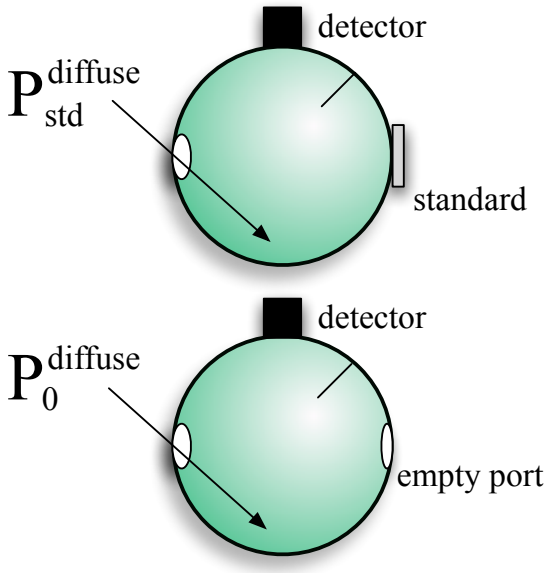

Figure 4: Diagrams of various measurements needed to determine the fraction of diffuse illumination f and the sphere parameter γ.

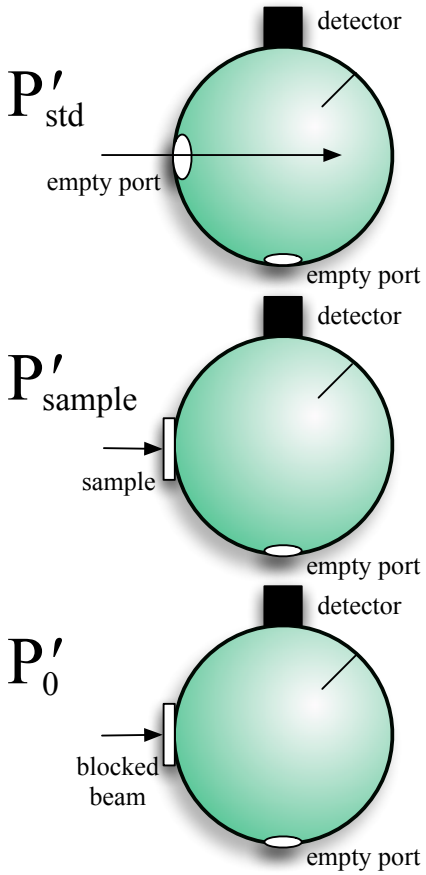

Figure 5: Diagrams of various integrating sphere transmission measurements that are needed. The empty port on the bottom of the spheres should be identical to the size of the entrance port in the sphere reflection measurements.

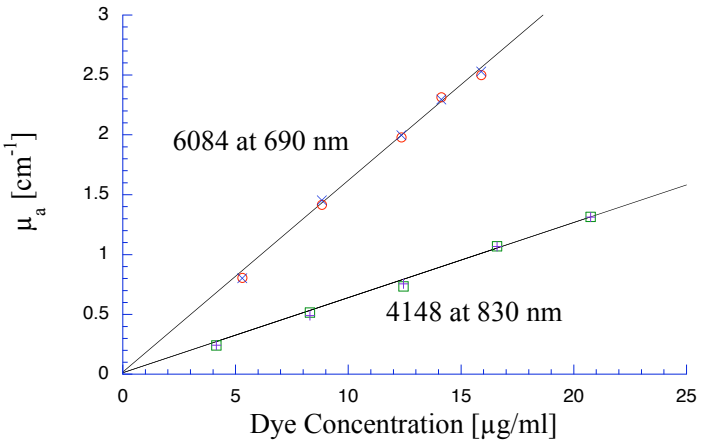

Figure 6: The absorption coefficient at 690 nm as a function of dye concentration of Epolight 6084 in polyurethane 1 week (X) and 1 year after casting (circles). The fitting line is $\mu_a^{690} = a_1 C_{6084} + \mu_{a0}^{690}$, where $a_1 = 0.16\,\mathrm{cm}^{-1}\mathrm{mL}/\mu\mathrm{g}$ and $\mu_{a0}^{690} = 0.019\,\mathrm{cm}^{-1}$ is the absorption coefficient for polyurethane at 690 nm after 1 year. The absorption coefficient at 830 nm is also shown as a function of dye concentration of Epolight 4148 in polyurethane 1 week (+) and 1 year after casting (squares). The fitting line is $\mu_a^{830} = a_2 C_{4148} + \mu_{a0}^{830}$, where $a_2 = 0.065\,\mathrm{cm}^{-1}\mathrm{mL}/\mu\mathrm{g}$ and $\mu_{a0}^{830} = 0.013\,\mathrm{cm}^{-1}$ is the absorption coefficient for polyurethane at 830 nm after 1 year. The standard deviation for each data point is less than the dimensions of the marker with a typical value of $0.002\,\mathrm{cm}^{-1}$.

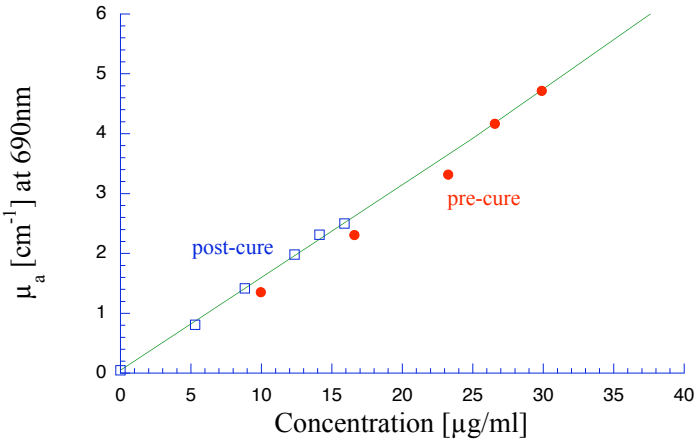

Figure 7: The absorption coefficient at 690 nm as a function of dye concentration of Epolight 6084 in part A of the polyurethane (circles) and after curing in polyurethane (squares). The fitting line is $\mu_a^{690} = a_1 C_{6084} + \mu_{a0}^{690}$, where $a_1 = 0.16\,\mathrm{cm}^{-1}\mathrm{mL}/\mu\mathrm{g}$ and $\mu_{a0}^{690} = 0.046\,\mathrm{cm}^{-1}$ is the absorption coefficient of polyurethane at 690 nm one week after casting.

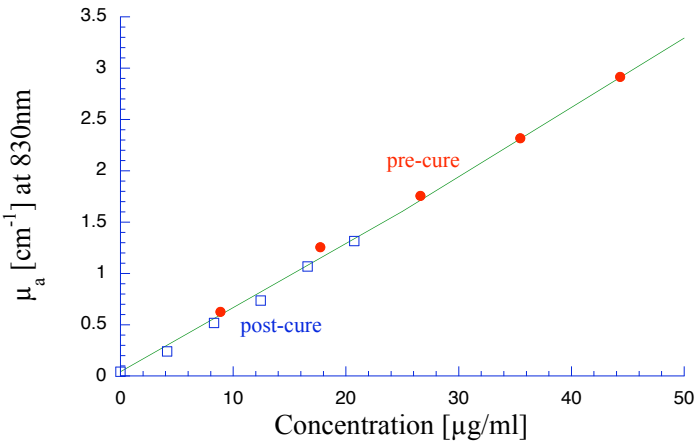

Figure 8: The absorption coefficient at 830 nm as a function of dye concentration of Epolight 4148 in part B of the polyurethane (circles) and after curing in polyurethane (squares). The fitting line is $\mu_a^{830} = a_1 C_{4148} + \mu_{a0}^{830}$, where $a_2 = 0.065\,\mathrm{cm}^{-1}\mathrm{mL}/\mu\mathrm{g}$ and $\mu_{a0}^{830} = 0.042\,\mathrm{cm}^{-1}$ is the absorption coefficient of polyurethane at 830 nm one week after casting.

.

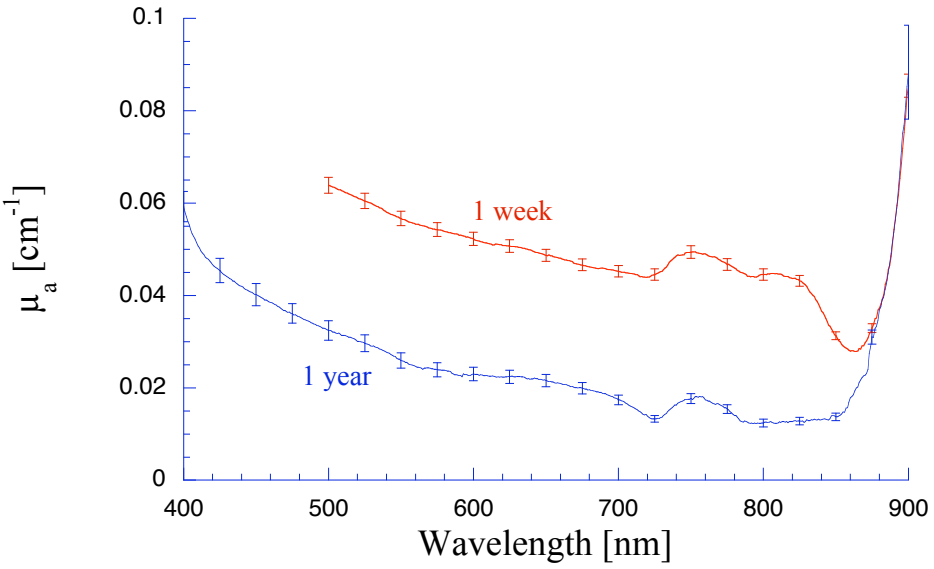

Figure 9: The absorption coefficient spectra of polyurethane 1 week and 1 year after casting the sample.

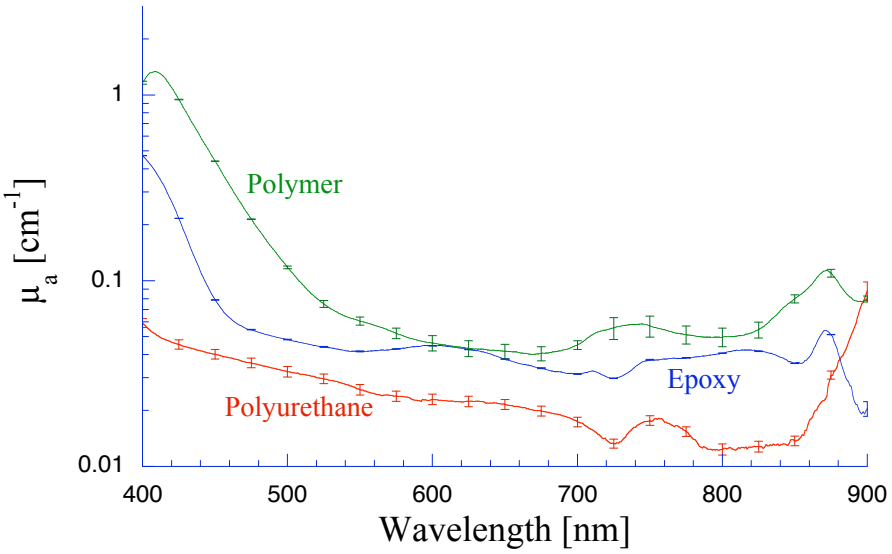

Figure 10: The absorption coefficient spectra of an epoxy resin, a polymer resin and a polyurethane one year after being cast.

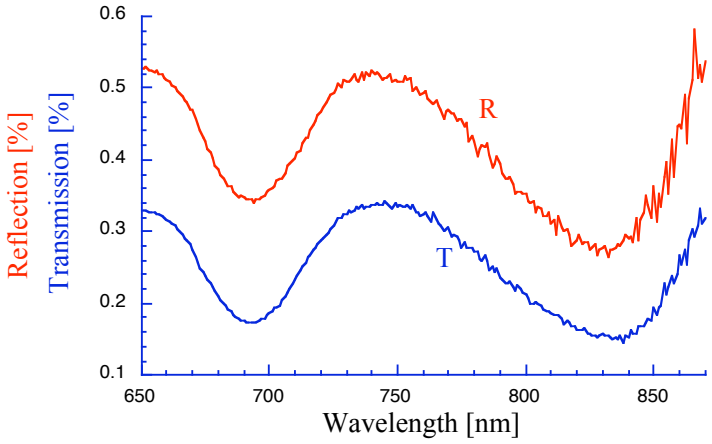

Figure 11: Typical reflectance and transmission measurements used to derive optical properties using the inverse adding-doubling method.

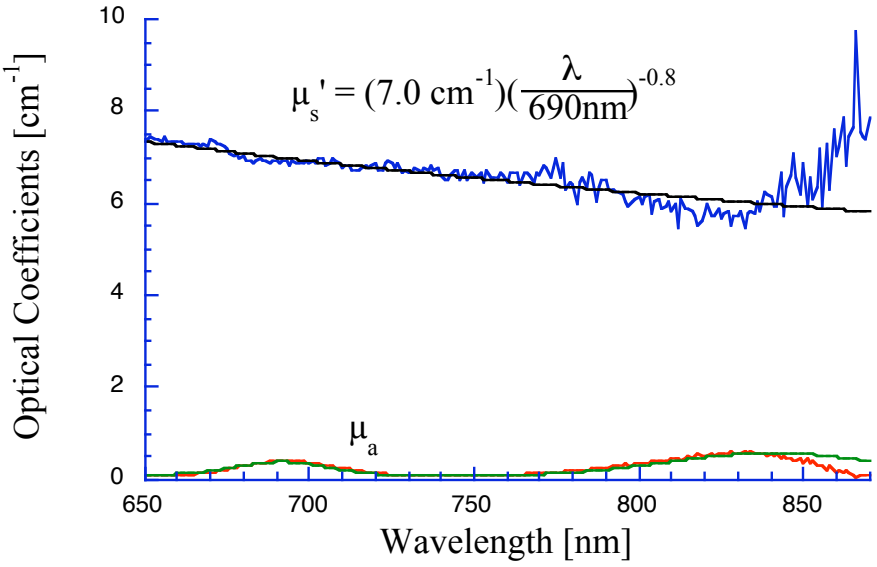

Figure 12: The reduced scattering and absorption coefficients spectra for the reflection and transmission data in figure 11 is shown in comparison to the spectrometer measurement of absorption for the same phantom made without added scatterer. The error bars are the standard deviation of three spectrometer measurements of different paths through the same clear phantom. Above 830 nm, the sensitivity of the detector drops precipitously causing error in the resultant optical properties.

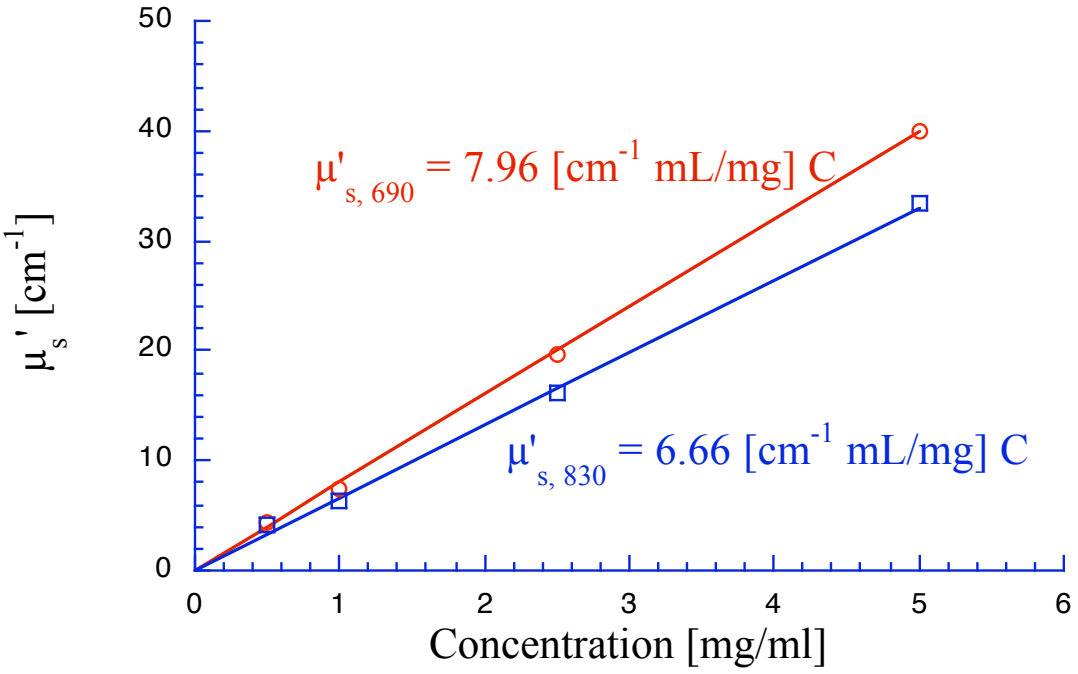

Figure 13: The scattering coefficient at 690 and 830 nm versus TiO_2 concentrations and their fitting lines. The mean particle size was 340 nm with a standard deviation of 90 nm. The average anisotropy for the particles is $g = 0.51$ at 690 nm and $g = 0.52$ at 830 nm using Mie theory.

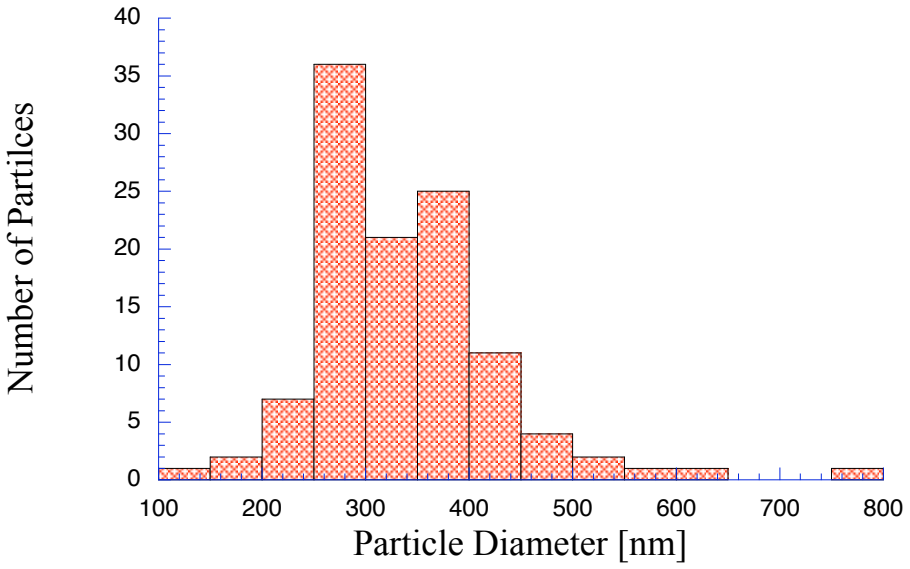

Figure 14: The size distribution of diameters of 112 titanium dioxide particles has a mean of 340± 90 nm.

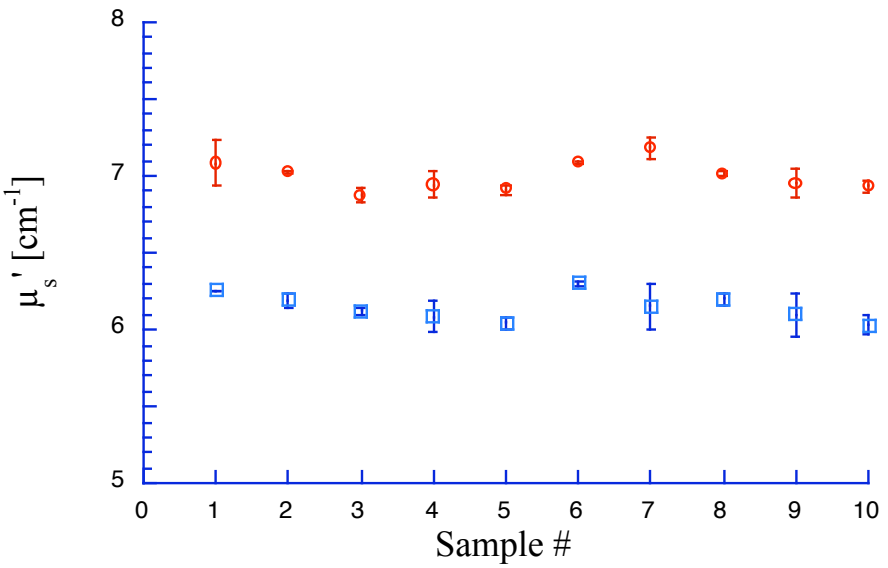

Figure 15: The variation in reduced scattering coefficient for ten different phantoms at 690 nm (circles) and 830 nm(squares) measured by the IAD method. All samples were designed to have the same reduced scattering properties. The error bars are the standard deviation of four sets or reflection and transmission measurements for each sample.

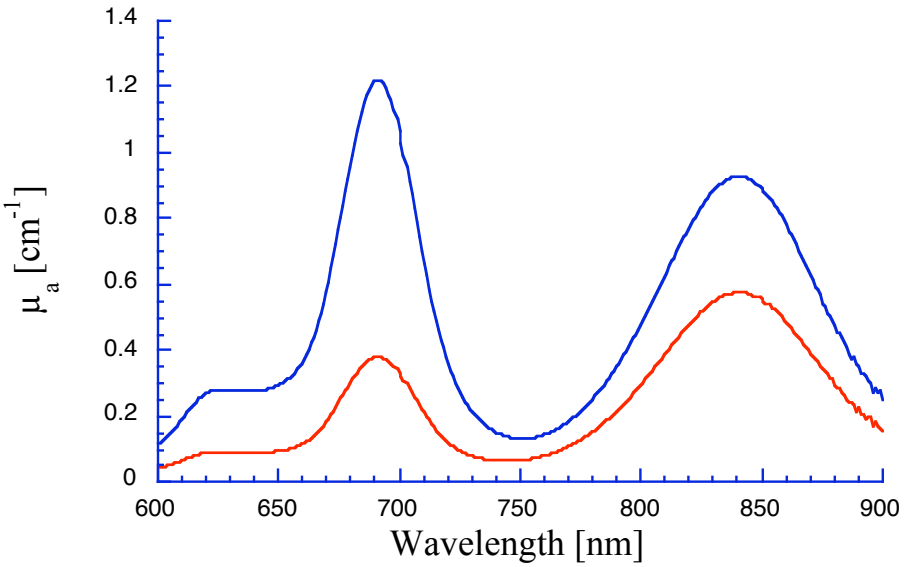

Figure 16: The absorption coefficient of two phantoms without titanium dioxide as measured by spectrometer.

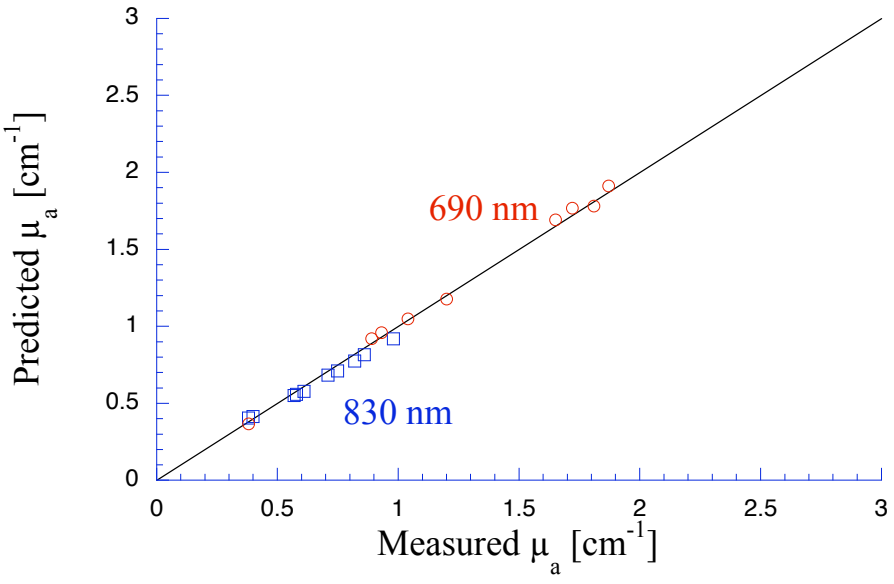

Figure 17: The predicted absorption coefficient using equations 1 and 2 are shown relative the spectrometer measured absorption coefficient for the ten different phantoms.

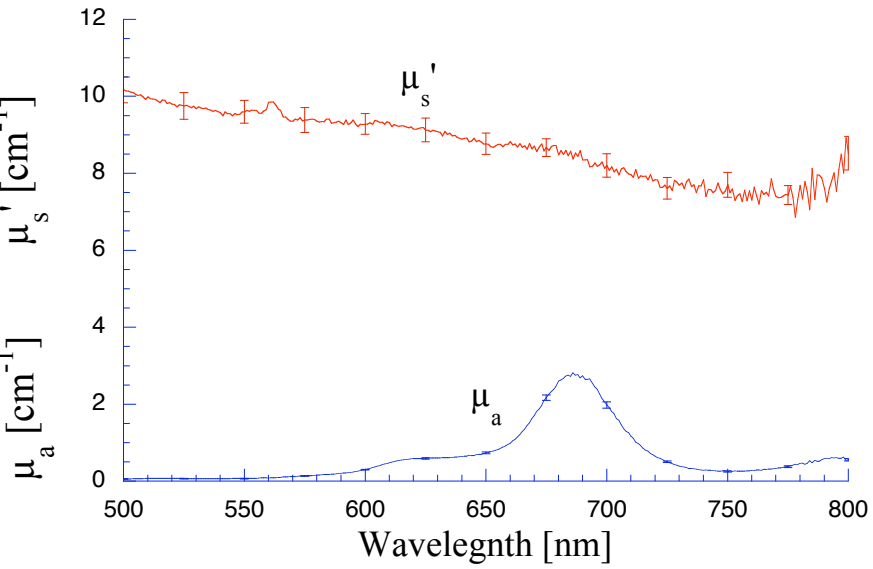

Figure 18: The absorption and reduced scattering coefficient spectra for twelve of the 20 identical phantoms. The error bars show the standard deviation for each optical property among the twelve phantoms and are approximately ± 3% between 600 and 800 nm.